606 621

October 14, 2002

TO: Waleed Abdalati, NASA Cryospheric Sciences Program Manager

FROM: Ted Scambos, NSIDC DAAC Research Scientist, principal investigator

Year 1 Report:

'Ice Shelves and Landfast Ice on the Antarctic Perimeter: Revised Scope of Work'

NASA Grant Number: NAG5-11308;

CU Grant Number: 1534620 (Speed type #48348)

Project Summary

Ice shelves respond quickly and profoundly to a warming climate. Within a decade after mean summertime temperature reaches ~0°C and persistent melt ponding is observed, a rapid retreat and disintegration occurs. This link was documented for ice shelves in the Antarctic Peninsula region (the Larsen 'A', 'B', and Wilkins Ice shelves) by the results of a previous grant under ADRO–1. Modeling of ice flow and the effects of meltwater indicated that melt ponding accelerates shelf breakup by increasing fracture penetration. SAR data supplemented an AVHRR- and SSM/I-based image analysis of extent and surface characteristic changes.

This funded grant is a revised, scaled-down version of an earlier proposal under the ADRO-2 NRA. The overall objective remains the same: we propose to build on the previous study by examining other ice shelves of the Antarctic and incorporate an examination of the climate-related characteristics of landfast ice. The study now considers just a few shelf and fast ice areas for study, and is funded for two years. The study regions are the northeastern Ross Ice Shelf, the Larsen 'B' and 'C' shelves, fast ice and floating shelf ice in the Pine Island Glacier area, and fast ice along the Wilkes Land coast. Further, rather than investigating a host of shelf and fast ice processes, we will home in on developing a series of characteristics associated with climate change over shelf and fast ice areas. Melt ponding and break-up are the end stages of a response to a warming climate that may begin with increased melt event frequency (which changes both albedo and emissivity temporarily), changing firn backscatter (due to percolation features), and possibly increased rifting of the shelf surface. Fast ice may show some of these same processes on a seasonal timescale, providing insight into shelf evolution.

Activities during Year 1

Monitoring of critical shelf areas continued using MODIS and AVHRR data, with supplemental images provided by Landsat 7, IKONOS, and the Radarsat RAMP 125-meter and 25-meter mosaics. The regions may be viewed, and images downloaded, at the NSIDC site at http://nsidc.org/iceshelves_images/index.html.

In February of 2002, a new cycle of retreat was noted in the Larsen B shelf, following indications of exceptionally warm temperatures in the Peninsula during the preceding months. Comparison of MODIS images from January 31 and February 17 indicated that several hundred square kilometers had rapidly calved, in the characteristic 'splinter' style of rapid ice shelf retreat. By March 17, over

3200 km2 of the shelf had been lost, essentially all of the shelf north of the line between Cape Disappointment and the Jason Peninsula.

The event provided an opportunity to re-examine the model of ice shelf retreat proposed by the PIs for this grant and Dr. Mark Fahnestock. The attached manuscript (written for SCIENCE but rejected; a revised version is accepted for Antarctic Research Series) details the work.

The most important result from this study is the identification of a relationship between ice shelf winter radar backscatter and the summertime melt season length that appears to be capable of identifying ice shelves on the verge of collapse. The basis for the relationship is that backscatter (determined from the RAMP 25m 1997 mosaic) increases with increasing seasonal melt, as meltwater seeps down into the firn and re-freezes. However, as the firn begins to saturate with ice (associated with longer and longer melt seasons, determined from passive microwave study), backscatter drops, due to the development of a smooth surface ice layer that specularly reflects the radar energy. This impermeable layer is a first requirement to support extensive melt ponding. The presence of melt ponds is key to breakup of the ice shelves, essentially representing a stored potential energy available for fracturing.

The grant also supported work related to a second paper, led by Dr. Douglas MacAyeal, that investigated the mechanism behind the catastrophic 'disintegration' portion of the breakup, i.e. the few-day period when the seemingly-integrated ice shelf becomes a large mass of separated bergs. This manuscript has been accepted by Journal of Glaciology.

In addition to ice shelf study, the grant funded planning activities for investigation of fast ice areas along the Wilkes land coast. Dr. Robert Massom is the co-investigator for this portion of the grant. Dr. Massom visited NSIDC for three weeks at the end of September, 2002, just after year one, but funded by the first year travel support money. This collaboration focussed on identifying MODIS and MISR images and algorithms that may be used to classify fast ice.

We continue to gather ice velocity data sets and ice elevation data in support of the two RAMP mappings. Additionally, the NSIDC PI attended two MAMM planning meetings, providing input on science objectives for the second mission.

<u>Plans for Year 2</u>

We will continue to monitor shelf areas and investigate the past history of other areas in Year 2. Further, we plan to submit a revised version of the Science manuscript that focuses on the melt-length/backscatter relationship and identifies key regions around the Antarctic that may be susceptible to breakup.

We also plan to conduct a major effort towards the fast ice analysis effort in Wilkes Land, during both Year 2 and a one-year extension of the grant. The extension will facilitate participation in a science cruise planned by the University of Tasmania and the Australian Antarctic Division in September – November 2003 using the Aurora Australis. The cruise is scheduled to visit an extensive fast ice area near Dumont D'Urville Station, making several in situ measurements.

Submitted to Science, June 7, 2002

Climate-induced Ice Shelf Disintegration in Antarctica

Ted Scambos[+], Christina Hulbe[*], and Mark Fahnestock[#]

Warming in the Antarctic Peninsula has caused the disintegration of several ice shelves. Loss of the northern Larsen B ice shelf in early 2002 typifies the pattern and pace of these events. Fracturing driven by meltwater occurs during extended melt seasons, leading to disintegration. Breakups over the last 20 years, coupled with prior stability over several millennia, show Peninsula climate is at its warmest now. Climate stability of ice shelves that ring Antarctica can be assessed using indicators that presaged Peninsula breakups, such as meltwater ponding. Disintegration via melt-driven fracturing occurs quickly once climate warms to the point of melt ponding.

Previous studies have considered the climatic limit of ice shelves (1, 2) and the possible role of meltwater in ice shelf breakup (3-5), but the rapidity of ice shelf retreat in the Peninsula, particularly the events of 1995 and 2002, has been a continuing surprise (Fig. 1). Although some Peninsula ice shelves have been retreating since the early 1970s and before (the Wilkins and George VI shelves), beginning about 1986 an increased rate of retreat was observed for all the northernmost ice shelves on the eastern and western Peninsula coast (Fig. 2) (6-9). Early retreat events were small, trimming a few kilometers

[+] National Snow and Ice Data Center, University of Colorado, Boulder, CO, 80309, USA
[*] Department of Geology, Portland State University, Portland, OR, 97207, USA
[#] Institute for the Study of Earth, Oceans, and Space, University of New Hampshire, Durham NH, 03824, USA

off the fronts of the shelves in warmer summers. However, a series of warm summers throughout the Peninsula in the 1990s precipitated larger, more catastrophic events.

In late January 1995, the Prince Gustav and Larsen A ice shelves disintegrated over the course of just a few days (10, 11). These shelves had slowly lost more than half of their historic extent prior to this event. The event introduced a new pattern of ice shelf disintegration, in which hundreds of square kilometers (1550 km^2 total) of shelf rapidly disaggregated to sliver-shaped, few-kilometer to sub-kilometer icebergs. Although similar patterns of shelf retreat had occurred before (12), the Larsen A event awakened glaciologists to the fact that climate-related processes could cause the near-instantaneous loss of entire ice shelves.

At the time of the Larsen A disintegration, a large tabular iceberg calved from the Larsen B (designated 'A32', initially 1720 km^2). This continued a pattern of quasi-periodic, ~50 year, calvings from this shelf (7). Up to this point, the Larsen B, further south than the other retreating ice shelves of the eastern Peninsula coast, had not experienced sustained retreat. However, in addition to the main calving, the northernmost portion of the shelf front (~550 km^2) broke up as smaller, elongate icebergs, in the manner of the retreating shelves to the north (11). At the end of these events the Larsen B had an extent similar to that in 1902, when it was first mapped, and to that inferred for ~1950, when an unobserved calving probably occurred (7). If the periodic, 'stable' cycle had continued, the shelf would have advanced eastward from this limit (roughly the line between the eastern tips of Robertson Island and the Jason Peninsula) and calved another large berg around 2045.

In a study of the stress and strain field of the Larsen B shelf, this line was identified as the minimum stable ice front position, represented by the easternmost transversely compressed ice in the shelf (the 'compressive arch') (13). In February, 1998, it was predicted (13) that the shelf would enter a breakup phase within a few years if this arch were disrupted. Just a few weeks later, a relatively small calving event, composed of sliver-shaped icebergs and sub-kilometer pieces, removed part of the compressive arch line (14).

Retreat of the front, while possibly a contributing factor to the breakup of the ice shelves, appears to be secondary to a more severe environmental influence: a profound climate warming. Surface air temperatures measured at several long-occupied research stations in the area show a mean temperature rise of 2.5°C over the last 5 decades (15–20) (Fig. 2). A number of proxy observations also indicate warming. Sea ice extent in the Bellinghausen Sea to the west of the Peninsula has decreased by 20% over the period 1979 – 1999 (21, 22), and both sea surface temperatures (23) and temperatures in the mid-ocean have risen (24). The air temperature rise and sea ice decline is observed for every season of the year. In summer, the warming has resulted in a gradual increase in the length of the melt season, rising approximately 1 day per year on average over the period 1978 – 2000 (25, 26). Causes of this warming are elusive. A complex relationship between temperatures, winds, and sea ice in this area and the Southern Oscillation has been identified (15, 27, 28), but a causal sequence among these climate indicators has yet to be established. Recently, circulation effects resulting from the seasonal loss of ozone has been proposed as a likely contributing factor (29).

As the melt season has lengthened, ponded meltwater has begun to appear on the northernmost shelves during mid- to late-summer. Melt ponds have been observed on the northern George VI shelf since the 1930s (30), but for the Larsen Ice Shelf they are a more recent occurrence. A review of late-summer Landsat and AVHRR images of the Larsen B from 1975 to the present tracks the frequency of melt ponding (Fig. 3, top); however, the image record is sparse for the earlier years. Comparing this record with mean summer air temperatures for nearby stations (Fig. 3) indicates that melt ponding on the Larsen B is associated with mean summer temperatures exceeding –1.5°C at the Marambio or Matienzo weather stations. Cooler years (1977, 1986, 1994, and 2001) show little or no ponding. Measured mean temperatures rarely exceeded –1.5°C prior to 1977 (17), and so we infer that melt ponds on the Larsen B must have been rare to unprecedented until the late 1970s (31). Further, the extent of ponding on the Larsen B has increased in recent years. Melt ponds were limited to the northwestern corner of the shelf in 1979 and 1988 (32). During the warmer summers of the 1990s the area marked by melt ponds gradually expanded to the Crane Glacier outflow and east (Fig. 1). By January 1998, summer melt ponds were present throughout the northern two-thirds of the shelf (from Cape Disappointment north to the Seal Nunataks), and from near the grounding line to the ice front.

After the events of January, 1995, the National Snow and Ice Data Center (NSIDC) began monitoring ice shelf activity in Antarctica using visible, near-infrared, and thermal satellite images (33). This time-series is useful for constraining the timing and causes of Peninsula ice shelf breakups, and for evaluating the stability of other shelves. Ice shelf retreat events, showing the sliver-iceberg calving style, were found to occur when ponded melt was present at or near the retreating ice shelf front. Disintegration occurred in ice that underlay the area of ponds. Timing of these events, in mid- to late austral summer, also implicated surface melt. The association of melt ponds with late-summer breakups was observed in a series of minor events on the Wilkins and Larsen B in the late 1990s, and with retrospective images acquired by NSIDC, in the George VI, Larsen A, Larsen Inlet, and earlier Wilkins events. Stable tabular-berg calving events do not show this seasonality, nor the co-location with meltponds (34, 35). The largest breakup events occur during the warmest summers, implying that ponded meltwater itself, and not associated winter re-freezing or other causes with less seasonality (e.g., sub-shelf ocean currents), is responsible (Fig. 3). Further, the sequence of ice shelves losing mass, beginning with the Wordie, Prince Gustav, and Larsen Inlet, and continuing with the Wilkins, Larsen A, and finally the Larsen B, follows the trend expected for an air-temperature related change; the warmest shelves are disintegrating first, then the next warmest, etc (6).

The associated change in calving style, in which the majority of ice is calved in small (~10 km^2 and less), often sliver-shaped icebergs, points directly to a change in fracturing style as the cause of collapse. Major calving events from stable shelves tend to be dominated by one or a few large tabular bergs. The January 1995 event on the Larsen B, consisting of a large tabular berg and a region of sliver-shaped crevasses, represents a transition from stable to unstable behavior.

This spatial and temporal association between melt ponds and breakup is clearly present in the February-March 2002 event on the Larsen B (Fig. 1). The differences in behavior between the northern and southern portions of the shelf are particularly illuminating. On January 31, satellite images revealed that the northern two-thirds of the Larsen B shelf was again extensively covered with melt ponds. In the following three weeks, subsequent images indicated that several ponds behind the northern shelf front area disappeared, while adjacent ponds remained visible. At the front, the calving rate of elongate, front-parallel icebergs increased significantly between January 31 and February 17, and an initial breakup event began. 632 km^2 were lost in this event, which, like earlier ones, was most active in the area near ponds. The southern portions of the shelf, where ponding was nearly absent, calved fewer, larger icebergs. By February 23 an additional 125 km^2 had calved. A March 5 image shows a loss of 1960 km^2 over the preceding 16 days, and a March 7 image reveals the loss of an additional 550km^2. By March 17 (image not shown), a total of 3373 km^2 of shelf had disintegrated, with the last 2500 km^2 occurring as a catastrophic disintegration. Extreme disruption of the shelf is indicated by the brilliant bluish color in the image, typical of the color of interior glacier ice. Further, moraine material, previously encased within the shelf, is visible as dark bands in the March 7 image. The lost shelf area lay almost completely within the region of scattered melt ponds indicated in the January 31 image.

Given the close association of surface melt ponding and ice shelf breakup, we used a numerical model of ice-shelf dynamics to evaluate processes by which meltwater could directly change ice-shelf behavior (7). The model incorporates ice thickness, input flux, the stress-strain relation for ice, termperature variations within the shelf, and geometry of the shelf at several stages of retreat, to determine stress field and flow speed. Comparison of modeled flow speed to observations was used to validate the model (9). A process in which surface fractures are extended downward by water pressure from infilling meltwater, previously discussed by Weertman, Hughes, and van der Veen (3-5), was identified as the most likely connection between the development of melt ponds and ice-shelf retreat (Fig. 4). In simulations of Larsen A and B, pre-existing crevasses deeper than 6 to 22 meters (depending on firn density), if filled 90% or more with water, were able to penetrate the ice shelf completely. This occurs because the extra pressure due to meltwater filling increases the stress intensity at the crevasse tip. If the sum of stresses acting on the tip meets or exceeds the fracture toughness of the ice (typically 30 to 80 kPa) (5), the crevasse propagates downward. Propagation halts when the lower surface of the shelf is breached or when tensile stress drops below the threshold value. The latter case would result from lowering of the water level in the crevasse. Thus a reservoir of meltwater, e.g., surface ponds, is required to maintain a water level of at least > 90% of the crevasse depth. A Landsat 7 image acquired during a previous warm summer season provides stunning evidence that this process is indeed operating on the shelf (inset on Fig. 1).

The melt-enhanced fracturing model requires pre-existing surface crevasses within the shelf. In mid-shelf ice where stresses are low, new crevasses are likely to form only near shear margins or the calving front; however, pre-existing crevasses do not close completely. This is the case for the thin slow-moving Peninsula shelves. Meltwater is acting on pre-existing crevasses carried out across the ice shelf by flow, and those crevasses remain partly open (bridged or snow-filled, but not healed) until meltwater filling occurs.

The persistence of the George VI shelf (which is only slowly retreating despite decades of abundant melt ponding) is evidence that shelves can tolerate extensive melt accumulation if new crevasses cannot form and old crevasses close due to compression. Extremely confined shelves, like George VI, or shelves where melting occurs in regions without surface crevasses, will not be susceptible to breakup. The Amery and Fimbul ice shelves are also examples of areas where extensive ponding occurs without shelf retreat. In both cases, melt ponds currently form in areas behind major obstructions to ice flow, where along-flow and across-flow tension is likely to be low (36).

While capable of explaining many observations, the melt-driven fracturing model alone is not sufficient to explain the most dramatic aspects of the January 1995 and March 2002 events. Neither the pre-existing crevasse density nor the volume of meltwater stored in surface ponds is likely to have been great enough to crack these shelves as rapidly and as finely as the final catastrophic collapses require. Instead, cumulative effects of melt-driven fracturing may result in ice shelves so unstable that additional processes beyond typical calving can occur. One explanation for the final catastrophic disruption of the shelves is a domino-like tipping of narrow intra-shelf blocks carved by closely-spaced fractures resulting from melt-driven fracturing (37).

The relationship between air temperature rise, increased surface melting, melt ponding, and ice shelf disintegration provides a set of remotely observable surface characteristics that can be used to evaluate any Antarctic ice shelf for susceptibility to the melt ponding – fracture enhancement breakup process. As demonstrated in Fig. 3, melt season length can be monitored by passive microwave emission changes. Radar or scatterometer data provides information on the firn structure and density. To support ponded water on the surface, the shelf firn must be impermeable. This occurs after repeated extensive melting events in which surface melt percolates down into porous snowpack and densifies it to the point of impermeability. This process has a profound effect on the post-melt-season radar backscatter of the upper few meters of the firn (38, 39). In areas of near-zero melting, snow is a weak absorber of radar-wavelength (~decimeter) energy, allowing it to penetrate deep within the snowpack with little backscatter to the radar receiver. However, with even modest amounts of melt, radar backscatter increases significantly due to coarse-grained, radar-reflective ice layers formed by refreezing of surface melt within the snowpack. Such regions are termed the 'percolation facies' of the ice sheet (39, 40). With increasing melt, percolation layering increases, and so radar backscatter increases, making some portions of the Greenland and Antarctic ice sheets among the highest backscattering surfaces on Earth. Brightness peaks when the firn saturates with melt layers, creating a solid, impermeable layer of ice. At this point, increasing melt smooths the upper surface, resulting in specular reflection of most of the radar energy. For non-nadir-looking radar instruments, this reduces backscatter by directing energy away from the receiver. We assume this *geographic* pattern of melt intensity versus backscatter is an *evolutionary* one as well for ice shelves in a warming climate (41).

The relationship of radar backscatter to surface melt season length clearly indicates the importance of firn impermeability for Antarctic ice shelves (Fig. 5). Although significant melt durations occur around much of the Antarctic perimeter, only the Peninsula shelves are at or approaching firn saturation. The three actively retreating shelf (Larsen B, Wilkins, and George VI) have the longest melt seasons on the continent, and significantly reduced backscatter. Regions adjacent to these areas, i.e., the southern Larsen B and northeastern Larsen C, have firn characteristics similar to the active-retreat shelves. With further warm summers, these areas will likely disintegrate via splinter-style calving, possibly catastrophically. The more southern parts of the Larsen C are nearly ice-layer saturated, but do not yet show reduced backscatter.

It follows from the melt ponding and melt-fracture-enhancement model that the climate stability limit of ice shelves is near the -1.5°C isotherm. This value and the model from which it is derived represent a distinction from previous estimates of the stability limit. Previous studies inferred either a 0°C summer (or January) limit (1, 42), or a –5°C mean annual temperature limit (43), from geography: no ice shelves were observed in areas exceeding these values. One explanation for the –5°C limit was a decrease in fracture toughness of ice as it nears the melting point (2). For the 0°C limit, the hypothesis was that the ice shelf becomes nearly isothermal, and therefor soft and unstably deformable, by melt percolation into the annual winter cold wave beneath the summer surface (1). For the model presented here, mean annual temperature may be unimportant. Mean summer temperature and melt season length, impermeability of the firn, and the proximity of melt ponds to pre-existing crevasses are paramount to shelf stability.. This places several ice shelves much closer to a threshold of retreat and breakup than previously thought. Much of the Antarctic perimeter has very low mean annual temperatures (-15 to -25°C) but still experiences a significant melt season. Summer climate warming and melt season increases at the rate occurring in the Antarctic Peninsula could render several ice shelves susceptible to breakup in just a few decades. As illustrated in Fig. 5, the Amery, Fimbul, West, and Shackleton ice shelves are closest to this limit. To date, none of these shelves shows anything but ordinary cyclical calving behavior.

Ice shelves partially restrict glacier outflow (44). Once removed, the mass flux of glaciers draining towards the former shelves may increase faster than accumulation within their catchments. Further, meltwater percolation can act on glaciers to increase their flow speed still further, by reducing the bed resistance to flow. Glaciers formerly feeding the Larsen A increased flow speed by 50% since its breakup (45). This raises the significance of ice shelf disintegration from that of a passive indicator of climate change to a possible step in raising sea level (1). Ice mass stored on the Peninsula is insignificant in terms of sea level increase, but this is not the case with other ice shelves. Of particular concern is the Ross Ice Shelf, into which substantial portions of the West and East Antarctic ice sheets flow, each containing ice equal to several meters of sea level rise. At present, only the northeastern-most portion of the Ross Ice Shelf experiences frequent (>1 day per year on average) melting, and backscatter values are relatively low.

Glaciological and geological evidence suggests that the current warming causing the shelf retreats in the Peninsula is unusual to unprecedented in the Holocene epoch. Formation of the largest retreating shelves, with flow-related features from grounding line to ice front, requires several centuries, and so summer temperatures must have been below the breakup threshold for that period (7). Sediments in the seabed beneath the former shelves provide a longer-term perspective. Coarse till-like layers of uniform provenance are interpreted as sub-glacial tills from a thicker ice sheet in the past. Layers of fine-grained, biogenic-rich material with high depositional rates, or dropstones of mixed provenance, are interpreted to mean that bays were open-water or seasonally sea-ice-covered in the past. In the case of the Prince Gustav and Larsen A, a few such layers within sediment cores indicate these areas were likely open water 2000 to 5000 YBP, and possibly 700 to 1500 YBP as well (46-48). However, sediment cores acquired from the embayed area in front of the Larsen B in 2002 show no such layers in preliminary analysis (48). This is interpreted to mean that, until the present warming, this shelf had not disintegrated since the Last Glacial Maximum, 12,000 YBP.

FIGURE CAPTIONS

Fig. 1. Satellite images of the breakup and surface melt ponding on the Larsen B ice shelf. Color images are from Channel 1 (red, 250 meter pixel scale), Channel 4 (green, 500 meter pixel scale) and Channel 3 (500 meter pixel scale) of the Moderate Resolution Imaging Spectrometer (MODIS) sensor on the Terra satellite. Ponded meltwater shows as dark blue spots in the January 31 image, organized into linear patterns by subtle flow-related features on the shelf surface. The dotted blue line shows the extent of disintegration on March 7, 2002, almost exactly enclosing the region of extensive ponding. Inset images in lower left track the disappearance of melt ponds in the weeks prior to breakup. Circled in green are ponds that survived the 23-day period after January 31; in red and blue are ponds that disappeared by February 17 and February 23, respectively. We interpret the disappearance as due to cracking and draining in the weeks prior to the main disintegration in early March. The Landsat 7-derived inset in the upper right provides a high-resolution view of the surface (15 meter pixel scale) in a previous summer, showing filled and drained ponds and water-filled cracks covering the surface.

Fig. 2. Map of the Antarctic Peninsula showing climate trends for selected stations and total breakup extents in square kilometers for seven ice shelves fringing the Peninsula. Station trends are reported in °C per decade, spanning the last ~45 years (13), except for Marambio, where records extend back only to 1971 (18, 50). These indicate an intense climate warming trend over the entire peninsula area, but not extending to the surrounding portions of Antarctica. Breakup areas (in km^2) and percentages (6, 7, 9, 11) indicate loss of shelf by retreat-style calving since 1980, exclusive of areas that would be expected to calve under steady-state conditions.

Fig. 3. Trend of climate, melting, and retreat in the northeastern Antarctic Peninsula ice shelves over the last three decades. Mean summer temperature trends are shown for three stations: Marambio (64° 14' S, 56° 37' W); Matienzo (64° 59' S, 60° 04' W) and Larsen AWS (66° 57' S, 60° 54' W) (18, 49). Melt days per year for a 25 km by 25 km area in the central Larsen B are derived from satellite passive microwave observation (26). For the melt season of 1988, an estimate of 20 additional days was added to account for a lack of satellite coverage from December 3, 1987 to January 12, 1988. The summertime presence of melt ponds on the Larsen B was determined from satellite images. Breakup events are shown when the timing is known to within a single year. Several minor breakups of the Larsen A, Larsen Inlet, and Prince Gustav that occurred in the 1980s cannot be precisely determined. The Larsen B iceberg calving event of January 1995 is not included because it may not be related to climate-driven retreat (49).

Fig. 4. Cartoon representation of variables affecting propagation of surface crevasses. 1. With low, but non-compressive, resistive stresses, pre-existing crevasses neither close nor grow. This situation is typical for many thin ice shelves. 2. Lithostatic pressure limits the penetration of air-filled crevasses. 3. With sufficient water depth (small a), the lithostatic pressure is overcome. Combined with the resistive stress, the extra outward pressure due to water-filling can induce the fracture tip to propagate downward.

Fig. 5. a: RAMP image of Antarctica showing approximate backscatter intensity, with shelf locations used in b plotted as circles; b: Mean melt days per year versus backscatter intensity for shelf and ice sheet areas (51). Melt days are determined from passive microwave data by the XPGR method (26). RAMP image copyright Canadian Space Agency. Error bars indicate one-sigma errors.

References and Notes

1) J. H. Mercer, *Nature* **271**, 321 (1978).

2) C. S. M. Doake, D. G. Vaughan, *Nature* **350**, 328 (1991).

3) J. Weertman, *International Association of Scientific Hydrology (IASH) Publication* No. 95, 139 (1973).

4) T. Hughes, *Journal of Glaciology* **29**, 98 (1983).

5) C. J. van der Veen, *Cold Regions Science and Technology* **27**, 31 (1998).

6) D. G. Vaughan, C. S. M. Doake, *Nature* **379**, 328 (1996).

7) T. A. Scambos, C. Hulbe, M. A. Fahnestock, J. A. Bohlander, *Journal of Glaciology* **46**, 516 (2000).

8) P. Skvarca, *Annals of Glaciology* **17**, 317 (1993).

9) H. Rott, W. Rack, T. Nagler, P. Skvarca, *Annals of Glaciology* **27**, 86 (1998).

10) We use the informal geographic nomenclature adopted by Vaughan and Doake (1996) to divide the Larsen Ice Shelf. The Larsen 'A' extends from the Sobral Peninsula to Robertson Island; the Larsen 'B' refers to the shelf between Robertson Island and Jason Peninsula; the Larsen 'C' is the section between Jason Peninsula and Gipps Ice Rise. A far southern section, Larsen 'D', is not discussed in this paper.

11) H. Rott, P. Skvarca. T. Nagler, *Science* **271**, 788 (1996).

12) B. Lucchitta, C. E. Rosanova, *Annals of Glaciology* **27**, 41 (1998).

13) C. S. M. Doake, H. F. J. Corr, H. Rott, P. Skvarka, N. W. Young, *Nature* **391**, 778 (1998).

14) This event occurred between February 15 and March 22, 1998, and consisted of the removal of about 125 km^2 of shelf; publication date for Doake et al. (13) is February 19, 1998. For more discussion, see http://nsidc.org/iceshelves/larsenb1998.

15) D. G. Vaughan, G. J. Marshall, W. M. Connolley, J. C. King, R. Mulvaney, *Science* **293**, 1777 (2001).

16) D. G. Vaughan, C. S. M. Doake, *Nature* **379**, 328 (1996).

17) P. Skvarca, W. Rack, H. Rott, T. Ibarzábal y Donángelo, *Annals of Glaciology* **27** 628 (1998).

18) P. Skvarca, W. Rack, H. Rott, T. Ibarzábal y Donángelo, *Polar Research* **18**, 151-157 (1999); also P. Skvarca, personal communication, March 2002.

19) J. C. King, *Journal of Climate* **14**, 357 (1994).

20) J. C. Comiso, *Journal of Climate* **13**, 1674 (2000).

21) S. S. Jacobs, J. C. Comiso, *Journal of Climate* **10**, 697 (1997).

22) C. Parkinson, *Annals of Glaciology* **34**, in press (2002).

23) R. W. Reynolds, T. M. Smith, *J. Climate* **7**, 929 (1994).

24) S. T. Gille, *Science* **295**, 1275 (2002).

25) J. Ridley, *Geophysical Research Letters* **20**, 2639 (1993).

26) M. Fahnestock, W. Abdalati, C. Shuman, *Annals of Glaciolgy* **34** in press (2002).

27) R. Kwok, J. C. Comiso, *Journal of Climate* **15**, 487 (2002).

28) D. G. Vaughan *et al.*, Climatic Change, in press (2002).

29) D. Thompson, S. Solomon, *Science* **296**, 895 (2002).

30) J. M. Reynolds, *Polar Record* **20**, 425 (1981).

31) Melt ponds can form in sub-zero mean air temperatures because air temperature is generally lower than surface skin temperature, and because strong melt-albedo feedbacks help melt additional water once melting begins. During cooler periods within the summer, thin ice layers form over growing ponds, insulating them and still permitting light and energy to enter the melt below. In a study of melt season length for the continent, melt onset was determined to coincide with a mean monthly air temperature of –2.5°C, and severity of melt increased rapidly with temperature (52).

32) P. Skvarca, *Annals of Glaciology* **29**, 255 (1999).

33) NSIDC's satellite image archive is available at http://nsidc.org/iceshelves.

34) M. A. Lazzarra, K. C. Jezek, T. A. Scambos, D. R. MacAyeal, C. J. van der Veen, *Polar Geography* **23**, 201 (1999); see also the National Ice Center website at http://natice.noaa.gov/southbergs.html.

35) S. S. Jacobs, D. R. MacAyeal, J. L. Ardai Jr., *Journal of Glaciology* **32**, 464 (1986).

36) N. Young, G. Hyland, *Annals of Glaciology* **34**, in press (2002).

37) D. MacAyeal, T. Scambos, C. Hulbe, M. Fahnestock, *Journal of Glaciology*, in press (2002).

38) R. A. Bindschadler, P. Vornberger, *Remote Sensing of Environment* **42**, 167 (1992).

39) M. A. Fahnestock, R. A. Bindschadler, R. Kwok, K. Jezek, *Science* **262**, 1530 (1993).

40) C. Benson, *Cold Regions Research Engineering Laboratory Report* **70** (1962).

41) The relationship between melt season length and backscatter is likely dependent on accumulation rate as well, with areas of greater accumulation requiring longer melt

seasons to achieve a given backscatter level. However, much of the perimeter of Antarctica has a moderate accumulation rate, between 200 and 600 kg/m^2 (53).

42) G. de Q. Robin, R. J. Adie, *Antarctic Research* (Butterworths, London, 1964).

43) J. M. Reynolds, *British Antarctic Survey Bulletin* **54** 123 (1981).

44) C. L. Hulbe, A. J. Payne, *Antarctic Research Series* **77**, 201 (2001).

45) H. Rott, W. Rack, P. Skvarca, H. De Angelis, *Annals of Glaciology* **34**, in press (2002).

46) E. Domack, A. Leventer, R. Gilbert, S. Brachfeld, S. Ishman, A. Camerlenghi, K. Gavahan, D. Carlson, A. Barkoukis, *Eos* **82**, 13 (2001).

47) C. J. Pudsey, J. Evans, *Geology* **29**, 787 (2001).

48) E. Domack, personal communication, presentation at 'Antarctic Peninsula Climate Variability: A Historical and Paleoenvironmental Perspective', April 3-5, 2002.

49) Station temperatures are from the cited publication and personal communication from P. Skvarca, 2002, as well as from the University of Wisconsin Automated Weather Station website at (http://amrc.ssec.wisc.edu/aws). Melt pond presence/ absence is determined from Landsat browse images (http://edcsns17.cr.usgs.gov/ EarthExplorer) and AVHRR browse images (http://nsidc.org/iceshelves); ponding absence means no evidence of ponds in any clear-sky image acquired between January 1 and March 15 for that year.

50) Error in mean temperature trend for Marambio was estimated from comparison with errors and calculations in Comiso (17).

51) Backscatter values are determined by taking the mean of 2600 equally-spaced pixels (pixels represent a 25 m by 25 m area) over a 400 by 400 pixel subset (equivalent to a 10 km by 10 km region). Mean melt days per year are determined from a 21-year record of melt season length (1978–1999 exclusive of December-January of 1987/88). Zero melt in this period is plotted as 0.05 melt days per year (1 day in 20 years) on this graph. It is likely that the linear trend for moderate melting versus backscatter continues to the left of the graph, as shown in the inset.

52) H. J. Zwally, S. Fiegles, *Journal of Glaciology* **40**, 463 (1994).

53) D. G. Vaughan, J. L. Bamber, M. Giovinetto, J. Russell, A. P. R. Cooper, *Journal of Climate* **12**, 933 (1999).

54) T Scambos and M Fahnestock were supported by NASA Grant NAG5-11308 and NAG5-3438; C Hulbe by NSF-OPP grant 01-25754. Extensive, helpful discussions with Douglas MacAyeal, David Vaughan, Pedro Skvarca, and Eugene Domack contributed to the ideas presented here.

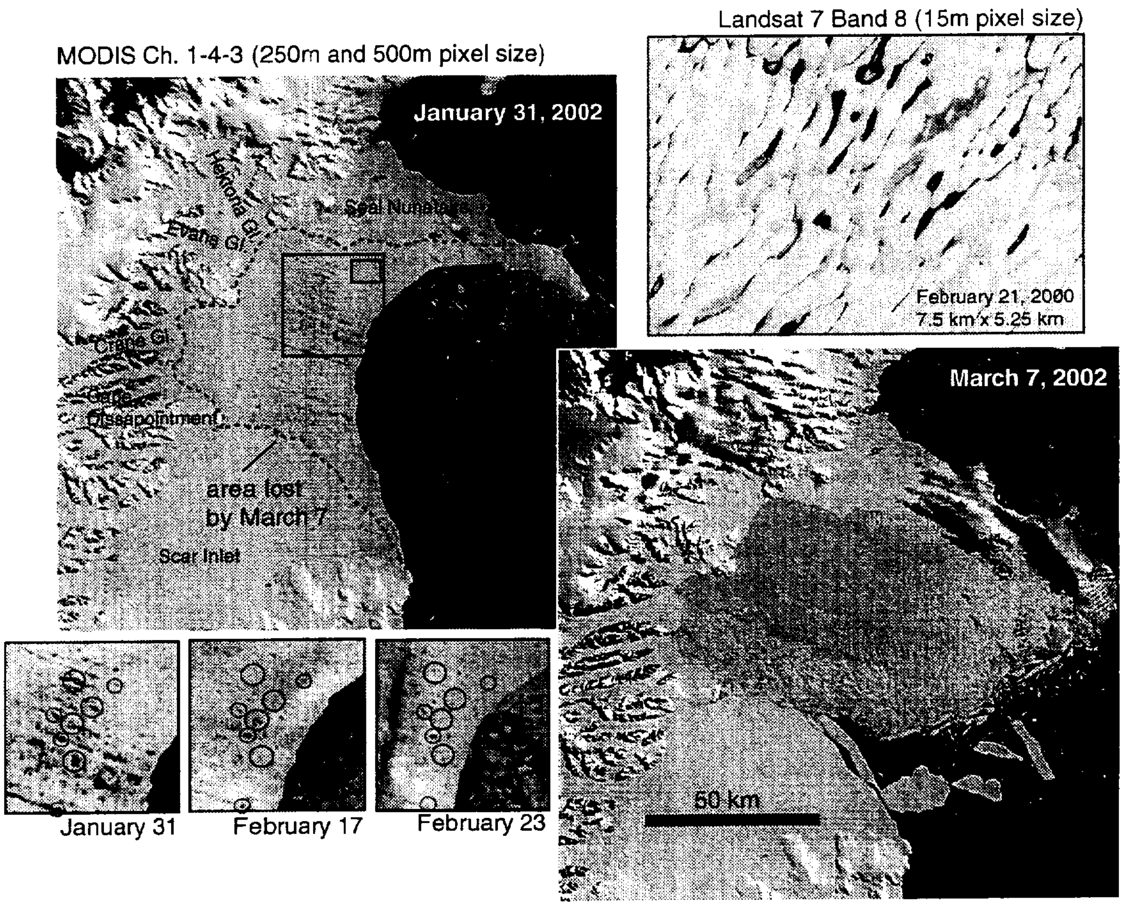

Scambos, Hulbe, Fahnestock Fig. 1
(suggest 2.5-column width for publication)

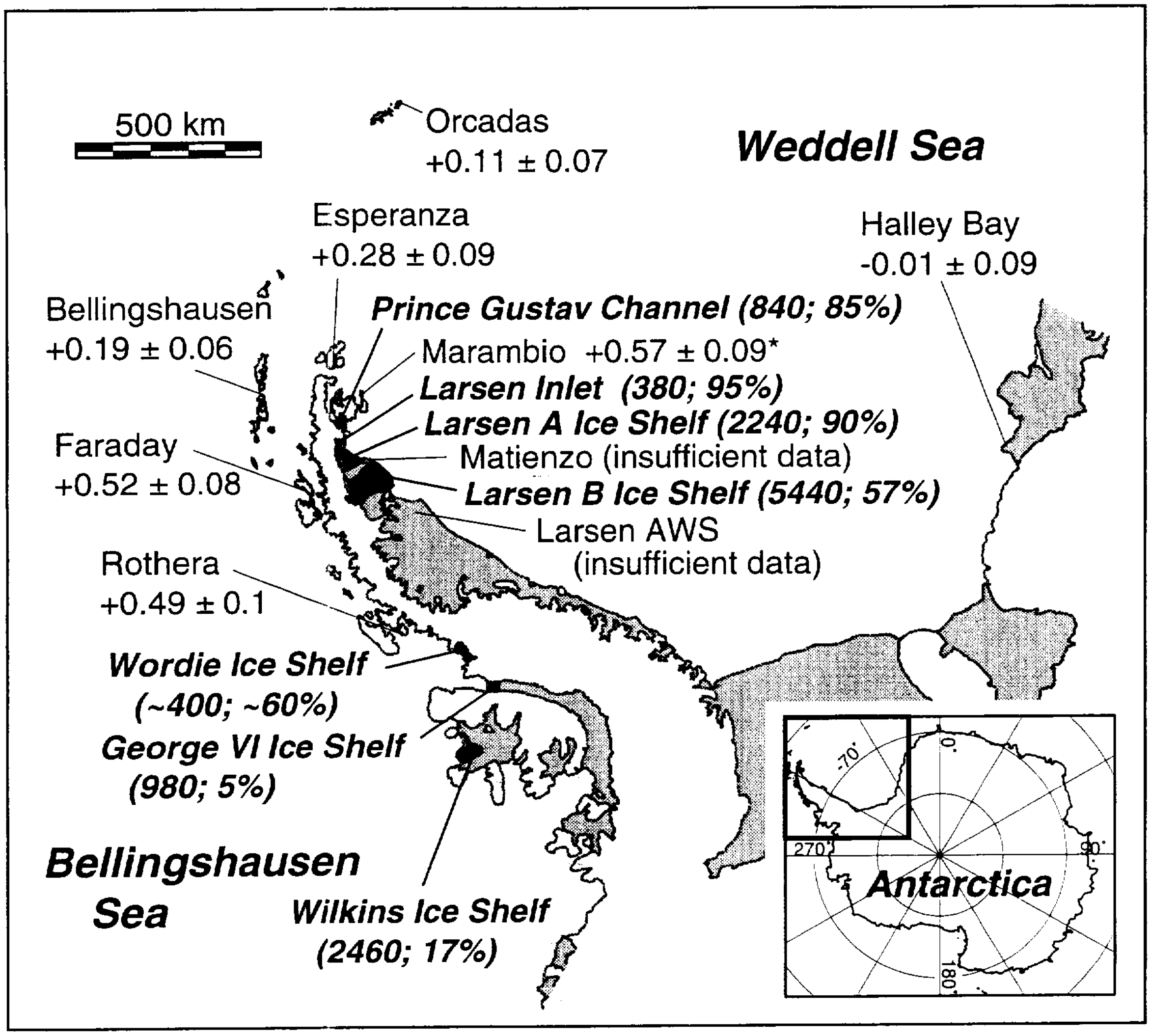

Scambos, Hulbe, Fahnestock Fig. 2
(suggest 1-column width for publication)

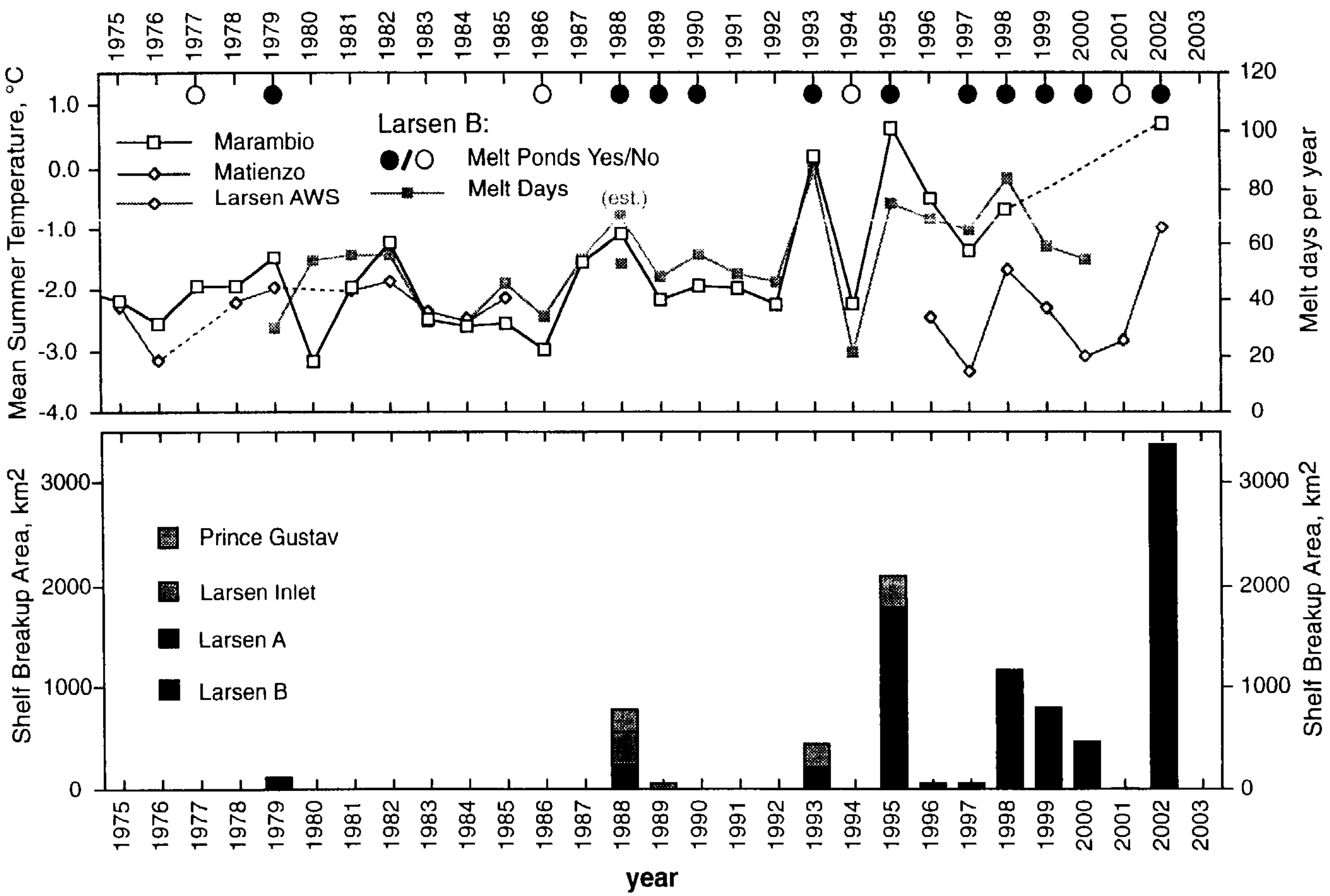

Scambos, Hulbe, Fahnestock Fig. 3
(suggest 1.5-column width for publication)

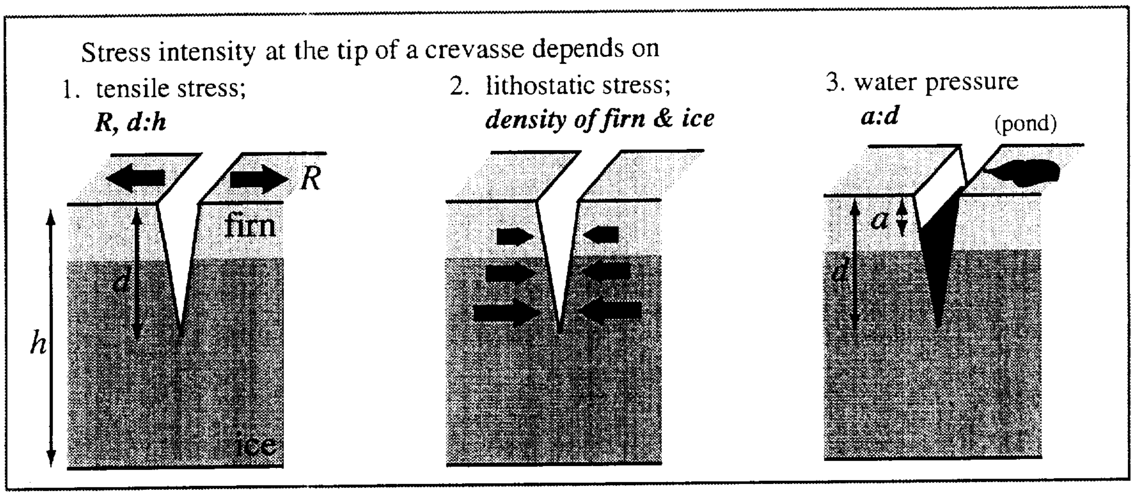

Scambos, Hulbe, Fahnestock Fig. 4
(suggest 1.5 column width for publication)

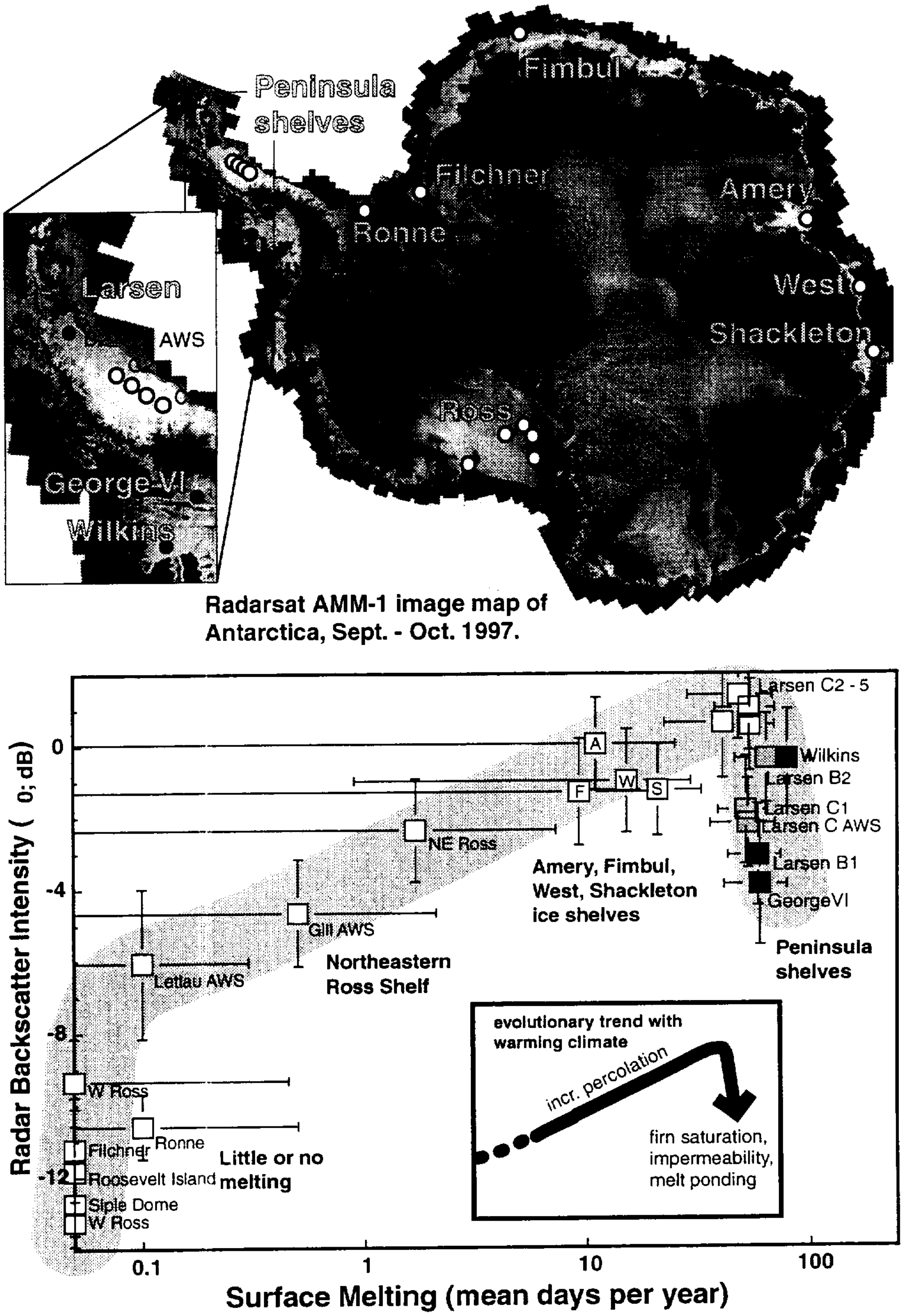

Scambos, Hulbe, Fahnestock Fig. 5
(suggest 1.5 column width for publication)